Quantitative Polar Representation of Left Ventricular Myocardial Perfusion, Function and Viability using SPECT and Cardiac Magnetic Resonance: Initial Results

Peter Cain, Martin Ugander, John Palmer, Marcus Carlsson, Einar Heiberg, Håkan Arheden

Department of Clinical Physiology, Lund University Hospital, Sweden.

Short title: Quantitative Polar Plots from cardiac SPECT and CMR

Corresponding author:

Associate Professor Håkan Arheden, MD, PhD

Department of Clinical Physiology

Lund University Hospital

Lund, SE-22185, Sweden

Tel: +46 46 173328

Fax: +46 46 151769

E-mail: hakan.arheden@med.lu.se

Summary

BACKGROUND: The clinical management of patients with coronary artery disease (CAD) often involves a complex assessment of the extent and severity of changes in left ventricular (LV) myocardial perfusion, function and viability. We aimed to explore the feasibility of integrative quantitative representation of LV perfusion, function and viability in adjacent polar plots. In order to assess the clinical usefulness of the quantitative methods, we also explored the relationship and determined the agreement between visual scoring and quantitative measurement of regional perfusion and function. METHODS: Ten patients with CAD underwent rest and stress 99m-Tc-tetrofosmin single photon emission computed tomography (SPECT) and cardiac magnetic resonance (CMR) imaging. Software was developed in-house for generating polar plots from semi-automatic quantification of rest and stress perfusion from SPECT, function from cine CMR and viability from delayed contrast enhancement (DE) CMR. The agreement between visual assessment and quantification of both perfusion and function was tested by Kendall's coefficient of concordance (W). RESULTS: Polar plots were created using quantitative data from the semi-automatic analysis of perfusion, function and viability. Kendall's W for agreement between quantitative measurement and visual scoring was 1.0 ($p<0.001$) for perfusion and 0.85 ($p<0.001$) for function. CONCLUSIONS: Side-by-side quantitative polar representation of LV perfusion, function and viability is feasible and may aid in the complex assessment of these parameters. The agreement between quantitative measurement and visual scoring was very good for both perfusion and function.

KEYWORDS: quantification, visual, agreement, delayed enhancement, infarction

Introduction

The clinical management of patients with coronary artery disease (CAD) involves a complex assessment of the extent and severity of changes in left ventricular (LV) myocardial perfusion, function and viability (Borges-Neto & Shaw, 1999; Marwick *et al.*, 1999). Assessment of these LV attributes is usually performed in isolation using either echocardiography, single photon emission computed tomography (SPECT), or more recently, cardiac magnetic resonance (CMR) imaging. The use of a polar plot from tomographic images of the LV was initally implemented with SPECT (Garcia *et al.*, 1985). Polar representation has proven to be a clinically useful method for displaying data from the whole LV in one image (Klein *et al.*, 1990; Altehoefer *et al.*, 1992). However, information in the literature on approaches to integrate information from SPECT and CMR are sparse (Faber *et al.*, 1991; Nelson *et al.*, 2004; Aladl *et al.*, 2004). Importantly, no previous approaches have undertaken side-by-side presentation of information on perfusion, function and viability as polar plots.

Gated SPECT and CMR can both be used to assess perfusion and function (Klocke *et al.*, 2003; Pennell *et al.*, 2004). CMR is considered the gold standard for assessment of function due to higher spatial and temporal resolution compared to gated SPECT (Persson *et al.*, 2005). Furthermore, SPECT is a well-established technique for assessing perfusion whereas CMR perfusion assessment has not yet been established in clinical routine (Pennell *et al.*, 2004). There are several software packages available for the semi-automatic quantification of perfusion and/or function from cardiac SPECT (Van Train *et al.*, 1994; Germano *et al.*, 1997; Liu *et al.*, 1999; Germano *et al.*, 2000). However, these

packages do not provide the ability for users to modify the process of analysis or access the original quantitative data. We therefore sought to develop an integrated method for quantitative polar representation of data from regional myocardial perfusion from SPECT and regional myocardial function and viability from CMR. In order to assess the clinical usefulness of the proposed quantitative methods, we also explored the relationship and determined the agreement between visual scoring and quantitative measurement of regional perfusion and function.

Methods

Study design. The study was approved by the local ethics committee and all subjects provided written informed consent prior to enrollment. We prospectively recruited ten patients with a history of CAD who were scheduled for first time elective coronary artery bypass grafting (CABG). These patients underwent rest and stress SPECT imaging and CMR prior to surgery. One patient underwent the same imaging protocol one month after surgery for the purpose of illustrating clinical usefulness. The images obtained from the one patient after surgery were not used for comparison between visual and quantitative data. All CMR and SPECT images were analyzed using in-house developed software. Cine CMR and SPECT images were visually scored by an experienced reader. Visual scores for function (cine CMR) and perfusion (SPECT) were compared to the corresponding quantitative measures of function and perfusion.

SPECT Imaging. Rest and stress imaging were performed on separate days, 30 minutes after intravenous injection of a body weight adjusted dose (500-700 MBq) of ^{99m}Tc-tetrofosmin (Amersham Health, Buckinghamshire, UK). Stress imaging was undertaken using either pharmacological or exercise stress. Pharmacological stress employed 5 mg/ml adenosine (Adenosin Item®, Item Development AB, Stocksund, Sweden) infused at a rate of 140 μg/kg/min for 3 minutes before tracer injection, and continued for 2 minutes following injection. Exercise stress was performed using a bicycle ergometer with a minimum increase to 85% of the maximum predicted heart rate. The subject was imaged in the supine position with a dual head camera (ADAC Vertex, Milpitas, California, USA) in steps of 5.6 degrees, 32 projections, 50 s/projection, using a 64 x 64 matrix yielding a digital resolution of 5 x 5 x 5 mm. Iterative reconstruction using

maximum likelihood-expectation maximization (MLEM) was performed with a low-resolution Butterworth post filter with a cutoff frequency set to 0.6 of Nyquist and order 5.0. No attenuation or scatter correction was applied. Lastly, short and long axis images were reconstructed.

CMR Imaging. Left ventricular regional function and viability were imaged in the short and long axis planes. Imaging was commenced during end-expiratory breath hold using a 1.5T system (Magnetom Vision, Siemens, Erlangen, Germany) and an ECG-triggered cine gradient echo sequence (resolution 1.6 x 1.6 x 8 mm, gap 2 mm) (Engblom *et al.*, 2004). Myocardial viability was imaged using a delayed contrast enhancement (DE) sequence consisting of a segmented inversion recovery turbo fast low-angle shot sequence (Simonetti *et al.*, 2001) (resolution 1.6 x 1.6 x 8 mm, gap 2 mm, inversion time set to null normal myocardium). DE CMR imaging was commenced 20 minutes after intravenous injection of 0.2 mmol/kg body weight of an extracellular contrast agent (Magnevist®, gadopentetate dimeglumine, Gd-DTPA, Schering). This approach has been shown to enhance infarcted myocardium (Kim *et al.*, 1999) due to an increased tissue distribution volume of Gd-DTPA in infarcted regions (Tong *et al.*, 1993; Arheden *et al.*, 1999; Flacke *et al.*, 2001; Klein *et al.*, 2004).

Image analysis. For CMR images, the apex was defined at the time of imaging by commencing the short axis imaging with an apical slice that encompassed the apical tip of the heart. For SPECT, the apex was defined manually in a vertical long axis image, after which contiguous 10 mm thick short axis slices were re-sampled from the original short axis slices. All LV short axis slices were used to develop polar plots. Comparison of visual scoring and quantitative measurement was undertaken using 12 segments per slice

in four mid-ventricular slices in order to avoid partial volume effects at the apex and through-plane motion in the base of the left ventricle (figure 1). Quantification of perfusion, function and viability was performed along radial profiles from the geometric centroid of the left ventricular lumen at every second degree, yielding 180 measurements per short axis slice. For all LV attributes, 15 measurements (corresponding to 30 degrees) were averaged to obtain mean values for 12 segments per slice.

i) Analysis of perfusion.

For visual perfusion scoring, short axis rest and stress SPECT images were assessed independently, blinded to the corresponding rest or stress images and CMR results. Scoring was performed by an experienced reader using the 12 segment per slice, four slice model. Images were scored using the following scale: 0 = normal, 1 = mild perfusion abnormality, 2 = moderate abnormality, 3 = severe abnormality, and 4 = maximal abnormality (no perfusion). For quantitative measurement, the centroid of the left ventricular lumen was defined manually in each 10 mm thick short axis slice at rest and stress from SPECT. Images were manually cropped using a circular selection tool. From the centroid, perfusion was quantified as the area under the count density curve along a radial profile. The visually assessed transition between the myocardium and the blood pool typically ranged between 20-50% of the maximal count density in the same slice. In order to exclude measurement of counts from the blood pool, a cut off value of 30% of the maximal count density in the same slice was therefore chosen as the endocardial limit of the area under the curve measurement for each radial profile. All perfusion values were normalized, where the maximum uptake in the entire left ventricle was set to 100%.

ii) Analysis of function. Visual function scoring of cine CMR images was performed in consensus by two experienced readers blinded to both subject identity and DE CMR images. Function was scored using the 12 segment per slice, four slice model according to the following scale: 0 = normal, 1 = mild-to-moderate hypokinesis, 2 = severe hypokinesis, 3 = akinesis, and 4 = dyskinesis. Quantification of function was performed by measurement of wall thickening. Wall thickening was defined as the percent change in radial wall thickness between end diastole and end systole. End diastole and end systole were defined globally as the time frame in which the volume of the LV was largest and smallest, respectively. Endocardial and epicardial borders of the left ventricle were manually delineated in end diastole and end systole, excluding papillary muscles. Wall thickness in end diastole and end systole were quantified automatically along radial spokes emanating from the centroid of the endocardial delineation (figure 1) .

iii) Analysis of viability. Manual delineation was undertaken to define the endocardial and epicardial borders of the left ventricle and regions of hyperenhancement in DE CMR images. Quantification of viability was performed by measurement of infarct transmurality. Infarct transmurality was defined as the radial thickness of a region of hyperenhancement expressed as a percent of the total wall thickness in the same position. Infarct thickness and wall thickness were quantified automatically along radial spokes emanating from the centroid of the endocardial delineation (figure 1).

Generating polar plots.

Polar plots were generated using the quantitative data for perfusion, function and viability. All data was treated as polar coordinates (slice number as radius, segment position as angle) and subsequently converted to Cartesian coordinates for graphing as

polar plots. The quantitative value of perfusion, function or viability was represented in each polar plot by a color scale. The perfusion color scale was set to range between 0 and 100% of maximum LV perfusion on a per-patient basis. The wall thickening color scale was set to range between 0 and 100% of diastolic wall thickness on a per-segment basis. This was done because it has previously been shown using cine MRI that clinically discernable differences in wall thickening in patients with ischemic heart disease typically range between approximately 0 and 100% of diastolic wall thickness (Mahrholdt *et al.*, 2003). Wall thickening values less than zero were set to 0% and values greater than 100% were set to 100%. The infarct transmurality color scale was set to range between 0 and 100% infarct transmurality.

Statistics. Data are presented as mean +/- standard deviation (SD). Agreement between quantitative measurement and visual scoring of function and perfusion was tested by Kendall's coefficient of concordance (W). Kendall's W varies between 0, denoting no agreement, and 1 denoting maximal agreement. In the absence of accepted criteria for interpretation of the value of Kendall's W, the strength of agreement was interpreted using the same criteria as for interpretation of kappa as adapted by Altman: <0.20 = Poor, 0.21-0.40 = Fair, 0.41-0.60 = Moderate, 0.61-0.80 = Good and 0.81-1.00 = Very good (Altman, 1991). Comparison of visual scoring and quantitative measurements of both perfusion and function were undertaken using ANOVA with post hoc Bonferroni correction. A p-value of less than 0.05 was considered statistically significant.

Results

Polar plots. Figure 2 shows a representative case illustrating the feasibility of generating polar plots from SPECT and CMR studies of one patient undertaken both before and after three vessel coronary artery bypass grafting (CABG). Myocardium that is hypoperfused and hypofunctioning but viable can easily be identified and localised. Also, improvement in function and perfusion in viable regions after CABG can easily be assessed. See figure text for details.

Visual scoring and quantitative measurement of perfusion and function. Table 1 shows the patient characteristics for the 10 patients. Figure 3 shows the relationship between visual scoring and quantitative measurements of both regional perfusion from SPECT and regional function from cine CMR in 480 myocardial segments from 10 patients. All 480 myocardial segments were assessed with a visual perfusion score. 50/480 segments (10%) were not assessed with a visual function score due to poor image quality. Kendall's W for testing agreement between quantitative measurement and visual scoring was 1.0 ($p<0.001$) for perfusion and 0.85 ($p<0.001$) for function.

Discussion

This study has demonstrated that quantitative polar representation of LV perfusion, function, and viability is feasible and may provide a method for easy identification of hypofunctioning and hypoperfused but viable myocardium. Furthermore, quantitative measures of perfusion and function showed a very good agreement with visual scoring by experienced observers.

Clinical relevance of integrative representation of perfusion, function and viability. Management of ischemic heart disease is complex and often involves assessment of both myocardial perfusion, function and viability (Borges-Neto & Shaw, 1999; Marwick *et al.*, 1999; Kim *et al.*, 2000). Scintigraphic approaches are currently considered the mainstay of myocardial perfusion assessment (Klocke *et al.*, 2003) while echocardiography, and more recently CMR provide superior information regarding regional myocardial function (Pennell *et al.*, 2004). Furthermore, DE CMR has emerged as an accurate and robust tool for differentiating viable from infarcted myocardium (Kim *et al.*, 1999). Coordinated assessment of perfusion, function and viability can be challenging when applied in the scientific and clinical setting. The results from this study suggest that coordinated quantitative polar representation of perfusion, function and viability is possible and easy to compare (figure 2).

Relationship between visual score and quantitative measurement. There are two reasons to compare quantitative data with visual scoring. Firstly, there is an overwhelming body of data in clinical studies where visual scoring has been used to assess perfusion, function and viability. Secondly, a direct comparison between visual

scoring and quantitative measurement of perfusion and function has not yet been undertaken.

Perfusion. The relationship between quantification and visual scoring of the extent of a SPECT defect has previously been studied (De Sutter *et al.*, 2000), but to our knowledge, this is the first study to examine the relationship between visual and quantitative assessment of perfusion defect severity. The very good agreement between visual and quantitative perfusion suggests that the method of quantification is of clinical value.

Function. To date, little published data exists to establish the relationship between visual scoring of regional myocardial function by experienced readers and quantification of regional function from cine CMR. Our study found a very good agreement between visual scoring and quantitative measurement of function using Kendall's coefficient of concordance (W). The quantitative measure of function, however, differed significantly only between normal and abnormal visual scores. Similarly, quantitative echocardiograpic measures commonly struggle to separate grades of abnormality. Past echocardiographic studies have utilized a multitude of measures of radial myocardial function including various measures of endocardial displacement (Lang *et al.*, 1996; Cain *et al.*, 2002), myocardial thickening (Chan *et al.*, 2000), and Doppler based measures of intrinsic myocardial function (Tsutsui *et al.*, 1998). Taken together, these echocardiographic results suggest that quantitative measures often succeed in differentiating normal from abnormal function as defined by experienced readers. The reasons for this are unclear but may relate to the ability of the visual reader, purposefully or otherwise, to simultaneously assess multiple axes and features of regional function such as overall AV plane movement and normalization of thickening to 'normal'

segments within the same ventricle. Furthermore, quantitative measures do not typically take into account the significant normal inter-individual variation of radial myocardial function. Therefore, 'overlap' of quantitative measures between different visual function scores will inevitably occur (Ginzton *et al.*, 1986). Although we found a significant difference in quantitative function between normal and abnormal function, the discriminative ability of such quantitative approaches still appears to be somewhat unsatisfying due to the large inter-individual spread of values as previously discussed.

Limitations. CMR imaging is performed during breath hold and is time resolved over the cardiac cycle while SPECT images represent the average perfusion of the LV throughout all cardiac cycles during approximately 20 minutes of free breathing. Accurate alignment of tissue is hampered by these differences in temporal resolution in combination with differences in spatial resolution. The technique explored in this current study utilizes the similar alignment of the short axis images between imaging modalities and aligns the left ventricular myocardium based on anatomical landmarks. This technique to align CMR and SPECT images is similar in principle to that which has been previously described (Faber *et al.*, 1991; Nelson *et al.*, 2004; Aladl *et al.*, 2004). Furthermore, the observed good agreeement between visual scoring and quantitative assessment of perfusion and function may be related to the limited and selected group of patients.

Conclusions. Side-by-side quantitative polar representation of LV perfusion, function and viability is feasible and may aid in the complex assessment of these parameters. Quantitative measures and visual scoring of perfusion and function show a very good agreement with visual scoring by experienced readers.

Acknowledgments

This work was supported by research funding from the Swedish Research Council, Swedish Heart and Lung Foundation, Region of Scania and Lund University Faculty of Medicine.

References

Aladl UE, Hurwitz GA, Dey D, Levin D, Drangova M, Slomka PJ. Automated image registration of gated cardiac single-photon emission computed tomography and magnetic resonance imaging. *J Magn Reson Imaging* (2004); **19**: 283-290.

Altehoefer C, Kaiser HJ, Dorr R, Feinendegen C, Beilin I, Uebis R, Buell U. Fluorine-18 deoxyglucose PET for assessment of viable myocardium in perfusion defects in 99mTc-MIBI SPET: a comparative study in patients with coronary artery disease. *Eur J Nucl Med* (1992); **19**: 334-342.

Altman DG. *Practical Statistics for Medical Research*. London: Chapman & Hall; 1991.

Arheden H, Saeed M, Higgins CB, Gao DW, Bremerich J, Wyttenbach R, Dae MW, Wendland MF. Measurement of the distribution volume of gadopentetate dimeglumine at echo-planar MR imaging to quantify myocardial infarction: comparison with 99mTc-DTPA autoradiography in rats. *Radiology* (1999); **211**: 698-708.

Borges-Neto S, Shaw LK. The added value of simultaneous myocardial perfusion and left ventricular function. *Curr Opin Cardiol* (1999); **14**: 460-463.

Cain P, Short L, Baglin T, Case C, Bosch HG, Marwick TH. Development of a fully quantitative approach to the interpretation of stress echocardiography using radial and longitudinal myocardial velocities. *J Am Soc Echocardiogr* (2002); **15**: 759-767.

Chan J, Wahi S, Cain P, Marwick TH. Anatomical M-mode: A novel technique for the quantitative evaluation of regional wall motion analysis during dobutamine echocardiography. *Int J Card Imaging* (2000); **16**: 247-255.

De Sutter J, Van de Wiele C, D'Asseler Y, De Bondt P, De Backer G, Rigo P, Dierckx R. Automatic quantification of defect size using normal templates: a comparative clinical study of three commercially available algorithms. *Eur J Nucl Med* (2000); **27**: 1827-1834.

Engblom H, Hedstrom E, Palmer J, Wagner GS, Arheden H. Determination of the left ventricular long-axis orientation from a single short-axis MR image: relation to BMI and age. *Clin Physiol Funct Imaging* (2004); **24**: 310-315.

Faber TL, McColl RW, Opperman RM, Corbett JR, Peshock RM. Spatial and temporal registration of cardiac SPECT and MR images: methods and evaluation. *Radiology* (1991); **179**: 857-861.

Flacke SJ, Fischer SE, Lorenz CH. Measurement of the gadopentetate dimeglumine partition coefficient in human myocardium in vivo: normal distribution and elevation in acute and chronic infarction. *Radiology* (2001); **218**: 703-710.

Garcia EV, Van Train K, Maddahi J, Prigent F, Friedman J, Areeda J, Waxman A, Berman DS. Quantification of rotational thallium-201 myocardial tomography. *J Nucl Med* (1985); **26**: 17-26.

Germano G, Erel J, Lewin H, Kavanagh PB, Berman DS. Automatic quantitation of regional myocardial wall motion and thickening from gated technetium-99m sestamibi myocardial perfusion single-photon emission computed tomography. *J Am Coll Cardiol* (1997); **30**: 1360-1367.

Germano G, Kavanagh PB, Waechter P, Areeda J, Van Kriekinge S, Sharir T, Lewin HC, Berman DS. A new algorithm for the quantitation of myocardial perfusion

SPECT. I: technical principles and reproducibility. *J Nucl Med* (2000); **41**: 712-719.

Ginzton LE, Conant R, Brizendine M, Thigpen T, Laks MM. Quantitative analysis of segmental wall motion during maximal upright dynamic exercise: variability in normal adults. *Circulation* (1986); **73**: 268-275.

Kim RJ, Fieno DS, Parrish TB, Harris K, Chen EL, Simonetti O, Bundy J, Finn JP, Klocke FJ, Judd RM. Relationship of MRI delayed contrast enhancement to irreversible injury, infarct age, and contractile function. *Circulation* (1999); **100**: 1992-2002.

Kim RJ, Wu E, Rafael A, Chen EL, Parker MA, Simonetti O, Klocke FJ, Bonow RO, Judd RM. The use of contrast-enhanced magnetic resonance imaging to identify reversible myocardial dysfunction. *N Engl J Med* (2000); **343**: 1445-1453.

Klein C, Nekolla SG, Balbach T, Schnackenburg B, Nagel E, Fleck E, Schwaiger M. The influence of myocardial blood flow and volume of distribution on late Gd-DTPA kinetics in ischemic heart failure. *J Magn Reson Imaging* (2004); **20**: 588-593.

Klein JL, Garcia EV, DePuey EG, Campbell J, Taylor AT, Pettigrew RI, D'Amato P, Folks R, Alazraki N. Reversibility bull's-eye: a new polar bull's-eye map to quantify reversibility of stress-induced SPECT thallium-201 myocardial perfusion defects. *J Nucl Med* (1990); **31**: 1240-1246.

Klocke F, Baird M, Bateman T, Berman D, Carabello B, Cerqueira M, DeMaria A, Kennedy J, Lorell B, Messer J, O'Gara P, Russell RJ, St. John Sutton M, Udelson J, Verani M, Williams K. ACC/AHA/ASNC guidelines for the clinical use of cardiac radionuclide imaging: a report of the American College of

Cardiology/American Heart Association Task Force on Practice Guidelines (ACC/AHA/ASNC Committee to Revise the 1995 Guidelines for the Clinical Use of Radionuclide Imaging). *American College of Cardiology Web Site. Available at:* http://www.acc.org/clinical/guidelines/radio/rni_fulltext.pdf (2003).

Lang RM, Vignon P, Weinert L, Bednarz J, Korcarz C, Sandelski J, Koch R, Prater D, Mor-Avi V. Echocardiographic quantification of regional left ventricular wall motion with color kinesis. *Circulation* (1996); **93**: 1877-1885.

Liu YH, Sinusas AJ, DeMan P, Zaret BL, Wackers FJ. Quantification of SPECT myocardial perfusion images: methodology and validation of the Yale-CQ method. *J Nucl Cardiol* (1999); **6**: 190-204.

Mahrholdt H, Wagner A, Parker M, Regenfus M, Fieno DS, Bonow RO, Kim RJ, Judd RM. Relationship of contractile function to transmural extent of infarction in patients with chronic coronary artery disease. *J Am Coll Cardiol* (2003); **42**: 505-512.

Marwick TH, Shaw LJ, Lauer MS, Kesler K, Hachamovitch R, Heller GV, Travin MI, Borges-Neto S, Berman DS, Miller DD. The noninvasive prediction of cardiac mortality in men and women with known or suspected coronary artery disease. Economics of Noninvasive Diagnosis (END) Study Group. *Am J Med* (1999); **106**: 172-178.

Nelson C, McCrohon J, Khafagi F, Rose S, Leano R, Marwick TH. Impact of scar thickness on the assessment of viability using dobutamine echocardiography and thallium single-photon emission computed tomography: a comparison with

contrast-enhanced magnetic resonance imaging. *J Am Coll Cardiol* (2004); **43**: 1248-1256.

Pennell DJ, Sechtem UP, Higgins CB, Manning WJ, Pohost GM, Rademakers FE, van Rossum AC, Shaw LJ, Yucel EK. Clinical indications for cardiovascular magnetic resonance (CMR): Consensus Panel report. *J Cardiovasc Magn Reson* (2004); **6**: 727-765.

Persson E, Carlsson M, Palmer J, Pahlm O, Arheden H. Evaluation of left ventricular volumes and ejection fraction by automated gated myocardial SPECT versus cardiovascular magnetic resonance. *Clin Physiol Funct Imaging* (2005); **25**: in press.

Simonetti OP, Kim RJ, Fieno DS, Hillenbrand HB, Wu E, Bundy JM, Finn JP, Judd RM. An improved MR imaging technique for the visualization of myocardial infarction. *Radiology* (2001); **218**: 215-223.

Tong CY, Prato FS, Wisenberg G, Lee TY, Carroll E, Sandler D, Wills J, Drost D. Measurement of the extraction efficiency and distribution volume for Gd-DTPA in normal and diseased canine myocardium. *Magn Reson Med* (1993); **30**: 337-346.

Tsutsui H, Uematsu M, Shimizu H, Yamagishi M, Tanaka N, Matsuda H, Miyatake K. Comparative usefulness of myocardial velocity gradient in detecting ischemic myocardium by a dobutamine challenge. *J Am Coll Cardiol* (1998); **31**: 89-93.

Van Train KF, Garcia EV, Maddahi J, Areeda J, Cooke CD, Kiat H, Silagan G, Folks R, Friedman J, Matzer L, et al. Multicenter trial validation for quantitative analysis

of same-day rest-stress technetium-99m-sestamibi myocardial tomograms. *J Nucl Med* (1994); **35**: 609-618.

Tables

Table 1. Patient Characteristics

Age (years)	mean 65 +/- 5, range 60-77
Ejection fraction (%)	mean 48 +/- 10, range 33-64 [Å]
Male gender	10/10 (100%)
Single vessel disease	1/10 (10%)
Two-vessel disease	4/10 (80%)
Three-vessel disease	5/10 (50%)
Previous myocardial infarction	10/10 (100%)
Hypercholesterolemia	9/10 (90%)
Non-insulin dependent diabetes mellitus	2/10 (20%)
Insulin dependent diabetes mellitus	2/10 (20%)

[Å] one subject was omitted from mean ejection fraction calculation due to incomplete coverage of the left ventricle at imaging.

Figure Legends

Figure 1. Alignment of short axis slices between cardiac magnetic resonance (CMR) (upper) and ^{99m}Tc- single photon emission computed tomography (SPECT) (lower) images. The long axis image of the left ventricle (left) used to plan the appropriate short axis images (middle and right) are shown for both imaging modalities. All LV short axis slices were used to develop polar plots. The middle four short axis slices (heavy white lines) were used for examination of relationship between visual scoring and quantitative measurement. For CMR images, endocardial and epicardial images were outlined in end diastole (ED) and end systole (ES) to obtain wall thickening. Myocardial infarction (hyperenhanced region in middle row image) was manually delineated for measurement of infarct transmurality. Quantitative information was assessed every two degrees and averaged into a 12 segment model per short axis slice (middle). Visual scoring was undertaken using the same 12 segment model (right). For SPECT, a similar approach was used for quantitative measurement (middle) and visual scoring (right) of perfusion.

Figure 2. Example of polar plots generated from rest and stress ^{99m}Tc-tetrofosmin single photon emission computed tomography (SPECT) perfusion, resting function (wall thickening from cine cardiac magnetic resonance (CMR)), and viability (infarct transmurality from delayed contrast enhanced (DE) CMR) in one patient prior to, and six months after coronary artery bypass surgery (CABG). Perfusion is color coded according to a scale where 100% represents the maximum value in the left ventricle. Function is color coded according to a scale representing quantitative wall thickening defined as percent change in wall thickness between diastole and systole. Viability is color coded

according to a scale representing quantitative infarct transmurality (%), defined as the percent of the myocardial wall thickness that is hyperenhanced on DE CMR images. “I” indicates a region approaching transmural infarction that exhibits poor function and poor perfusion and does not improve in function after CABG. “H” indicates a region of hibernating myocardium characterized by lack of infarction, poor function and poor perfusion at rest and stress. The hibernating myocardium improves in both rest perfusion, stress perfusion as well as function after CABG. “S” indicates a region of stunned myocardium characterized by little or no infarction, poor function and reduced stress perfusion. The stunned myocardium improves in stress perfusion and function after CABG.

Figure 3. The relationship between visual scoring and quantitative measurement of perfusion (left) and function (right). The left panel shows data from ^{99m}Tc-tetrofosmin single photon emission computed tomography (SPECT) at rest (open circles) and stress (filled circles). The right panel shows percent wall thickening and visual function scores from cine cardiac magnetic resonance (CMR) at rest. Numbers represent myocardial segments per category and error bars denote one standard deviation. All visual perfusion scores differed significantly in quantitative perfusion ($p<0.001$ for all except *, denoting $p<0.05$ for the difference between rest perfusion scores 3 and 4). A normal visual function score differed significantly from all other scores. §§§ denotes $p<0.001$. Error bars denote SD.

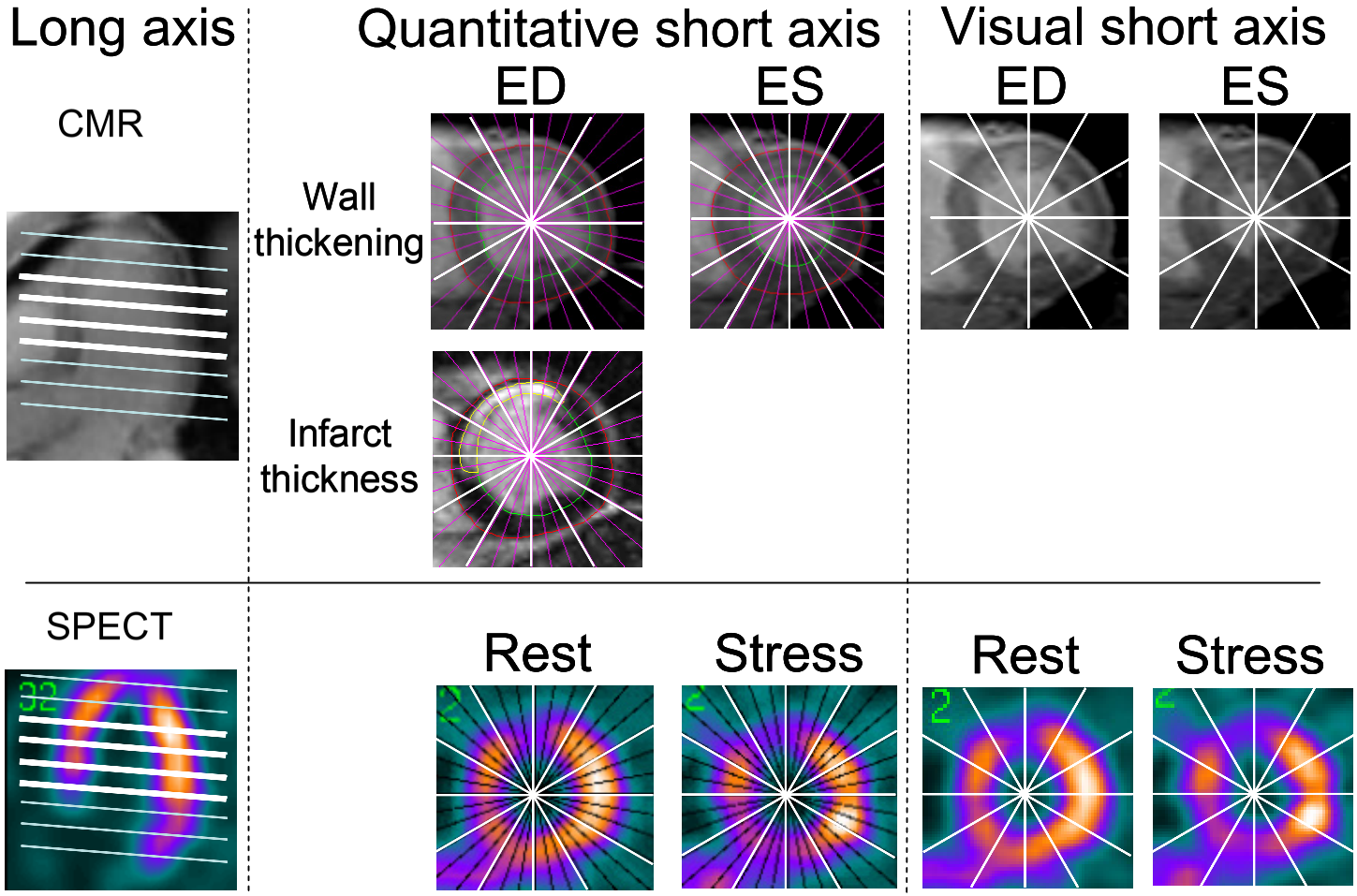
Long axis
Quantitative short axis
Visual short axis
ED
ES
ED
ES
CMR
Wall thickening
Infarct thickness
SPECT
Rest
Stress
Rest
Stress

Figure 1.

Figure 2

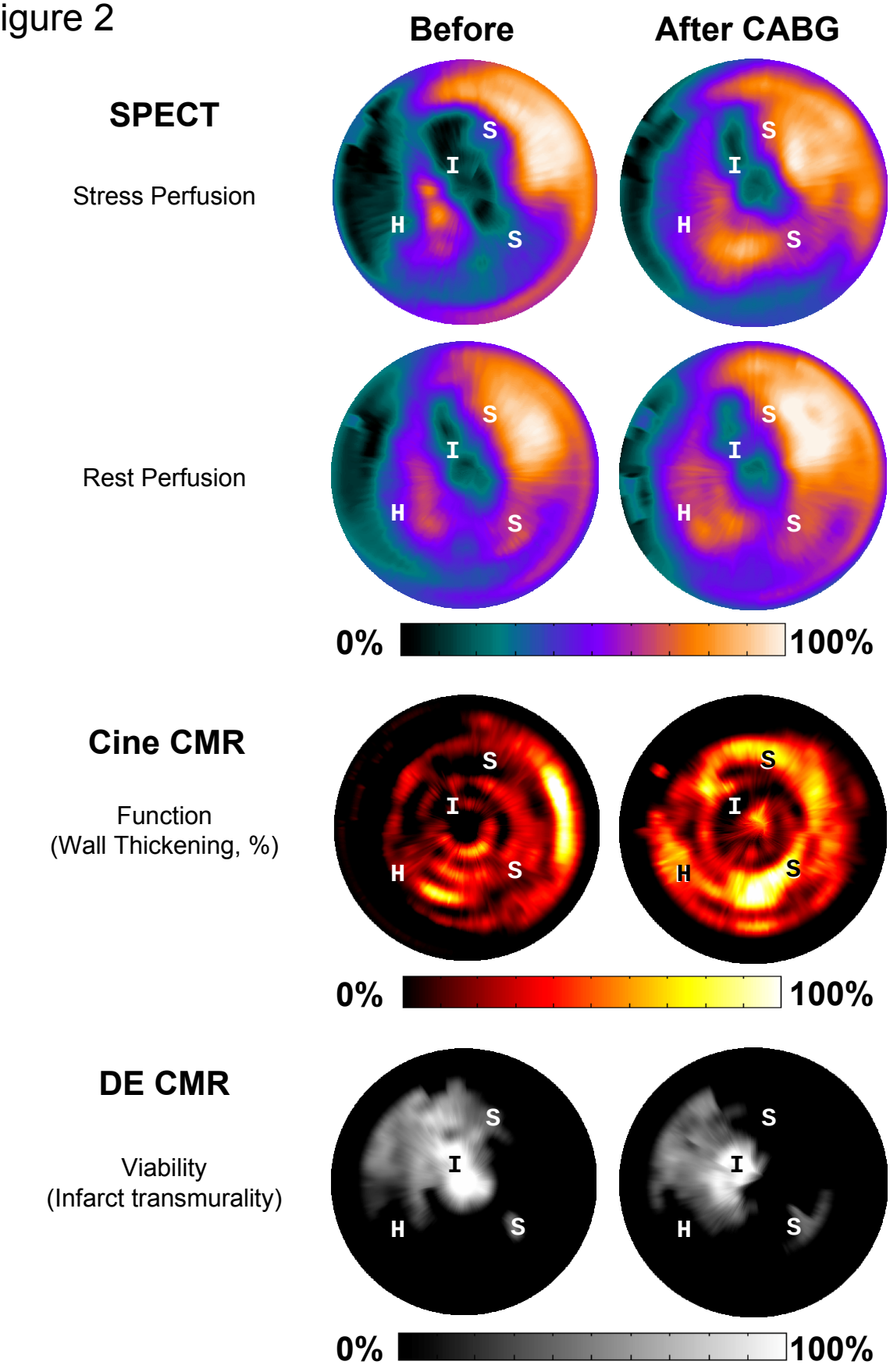
Before
After CABG
SPECT
Stress Perfusion
Rest Perfusion
S
I
H
S
0%
100%
Cine CMR
Function
(Wall Thickening, %)
DE CMR
Viability
(Infarct transmurality)

Figure 3

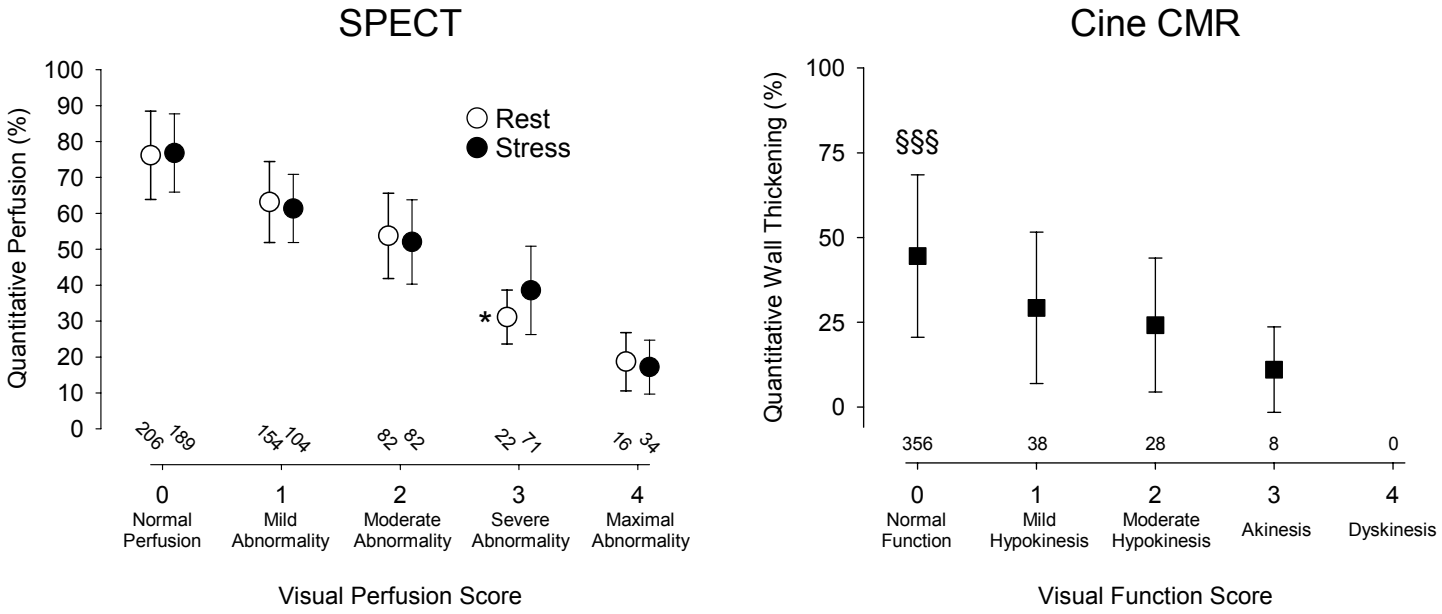
SPECT
Quantitative Perfusion (%)
100
90
80
70
60
50
40
30
20
10
0
Rest
Stress
*
206 189
154 104
82 82
22 71
16 34
0
Normal Perfusion
1
Mild Abnormality
2
Moderate Abnormality
3
Severe Abnormality
4
Maximal Abnormality
Visual Perfusion Score
Cine CMR
Quantitative Wall Thickening (%)
100
75
50
25
0
§§§
356
38
28
8
0
0
Normal Function
1
Mild Hypokinesis
2
Moderate Hypokinesis
3
Akinesis
4
Dyskinesis
Visual Function Score